S_1 Pedicle Subtraction Osteotomy in Sagittal Balance Correction. A Feasibility Study on Human Cadaveric Specimens

Vicente Vanaclocha[1], Amparo Vanaclocha-Saiz[2], Marlon Rivera-Paz[1], Carlos Atienza-Vicente[2], José María Ortiz-Criado[4], Vicente Belloch[3], José Manuel Santabárbara-Gómez[3], Amelia Gómez[3], Leyre Vanaclocha[5]

■ BACKGROUND: **A cadaveric feasibility study was carried out. Osteotomies to correct fixed sagittal imbalance are usually performed at L_3/ L_4.**

■ OBJECTIVE: **To investigate the feasibility of S_1 pedicle subtraction osteotomy to correct spinal deformity and spinopelvic parameters, achieving better results with more limited exposure. The data obtained will allow a fixation construct specific for this osteotomy to be designed.**

■ METHODS: **S_1 pedicle subtraction osteotomy was performed on 12 cadaveric specimens. Baseline and post-procedural computed tomography and biomechanical studies were performed. Data were analyzed with a fixation system SolidWorks model, and the redesigned fixation construct was described and analyzed with an ANSYS model.**

■ RESULTS: **S_1 pedicle subtraction osteotomy is technically feasible. The fixation can be achieved with L_4, L_5, and iliac screws connected with bars. The system can be reinforced with a polyetheretherketone cage placed anteriorly in the S_1 body osteotomy site, a cross-connecting bar, a double iliac screw, or an anterior interbody cage placed at the L_5-S_1 disc. The fixation strength is improved by angulating the iliac rod channel 10°, adding a semi-sphere to the locking screw contact surface and 2 fins to its saddle. The redesigned construct showed suitable stress and deformation levels, achieving the expected biomechanical requirements.**

■ DISCUSSION: **Compared with surgery on higher levels, S_1 pedicle subtraction osteotomy allows greater correction with shorter fixation, because the osteotomy is performed at a more caudal level, modifying the spinopelvic parameters.**

■ CONCLUSIONS: **S_1 pedicle subtraction osteotomy is technically feasible. Finite element analysis results indicate that it has appropriate biomechanical properties.**

INTRODUCTION

In the standing position, a straight vertical line (plumb line) must cross through the vertebral bodies of C_2, C_7, and S_1.[1,2] This is known as spinal sagittal balance.[3] Hence, sagittal imbalance[4] occurs when that vertical line is off center.[5-7] Compensatory mechanisms appear whenever the plumb line deviation is >5 cm[4] with pelvic retroversion[8] and hip and knee flexion,[9] forcing the spinal musculature to undergo early fatigue and pain.[1] In addition, ambulation is impaired, and the cervical

Key words
- Finite element analysis
- S_1 pedicle subtraction osteotomy
- Sagittal profile
- Spinal balance
- Spinopelvic alignment
- Spinopelvic parameters

Abbreviations and Acronyms
3D: Three-dimensional
ALIF: Anterior lumbar interbody fusion
CT: Computed tomography
FEA: Finite element analysis
LL: Lumbar lordosis
PEEK: Polyetheretherketone
PI: Pelvic incidence
PJK: Proximal junctional kyphosis
PSIS: Posterosuperior iliac spine
PSO: Pedicle subtraction osteotomy
PT: Pelvic tilt
S_2AI: S_2 alar-iliac
SD: Standard deviation
SPO: Smith-Petersen osteotomy
SS: Sacral slope

From the [1]Hospital General Universitario de Valencia, Valencia, Spain; [2]Instituto de Biomecánica, Valencia, Spain; [3]ERESA, Valencia, Spain; [4]Instituto de Medicina Legal de Valencia, Valencia, Spain; and [5]Medical School, University College London, London, United Kingdom

To whom correspondence should be addressed: Vicente Vanaclocha, M.D., Ph.D. [E-mail: vvanaclo@hotmail.com]

Citation: World Neurosurg. (2019) 123:e85-e102.
https://doi.org/10.1016/j.wneu.2018.11.052

*Journal homepage: **www.journals.elsevier.com/world-neurosurgery***

*Available online: **www.sciencedirect.com***

1878-8750/$ - see front matter

lordosis forces a horizontal gaze to be maintained, at times inducing neck pain.[10,11]

The primary goal for any spinal reconstructive surgery is restoration of sagittal balance.[2,4] Flexible deformities can be corrected with careful intraoperative positioning and maintained with fixation constructs,[2] whereas rigid or fixed deformities require osteotomies,[4,12,13] which have a significantly increased complication rate.[13] Even with osteotomies, only a third of patients reach a neutral spinal alignment and reoperations are common.[14-17]

Over the years, several osteotomies have been described: Ponte,[18,19] Smith-Petersen osteotomy (SPO),[20] pedicle subtraction osteotomy (PSO),[21] and vertebral column resection.[22] The SPO is the least aggressive and best tolerated but it usually applied to several segments because the correction is limited to 5°–10° per level.[20,23] Instead, the PSO allows 30°–40° of correction per level, has a bigger chance of bone fusion, and does not require a supplemental anterior approach.[24,25] However, it is associated with high rates of perioperative complications, which increase in frequency and severity with the comorbidities and extent of the fixation construct.[13-15,21,26,27]

Postoperative neurologic deficits are moderately frequent,[13,14] although most recover spontaneously.[13,14,28] Mechanical failure of the fixation construct is relatively common[15,26,29] and the reported 5-year reoperation rate is 25%.[14,30] Some surgeons have recommended associating the PSO with several SPOs at other levels instead of a second PSO.[27] Vertebral column resection achieves the maximum degree of deformity correction, but it is particularly risky for elderly people.[2,31,32]

A retroperitoneal anterior intersomatic cage combined with a posterior fixation system can be used[33-35] to reduce the number of levels to be fused. However, this technique requires both an anterior and a posterior approach, and when applied to elderly people, it is associated with high morbidity and mortality.[33,34]

The PSO has become exponentially popular to correct fixed sagittal imbalance.[14] The perfect circumstances for this technique are 10–12 cm sagittal imbalance, a sharp angular kyphosis, or multilevel circumferential fusions.[4,36] PSO entails removing both pedicles plus a vertebral body wedge[37] and gradually extending the operating table.[37] It is performed

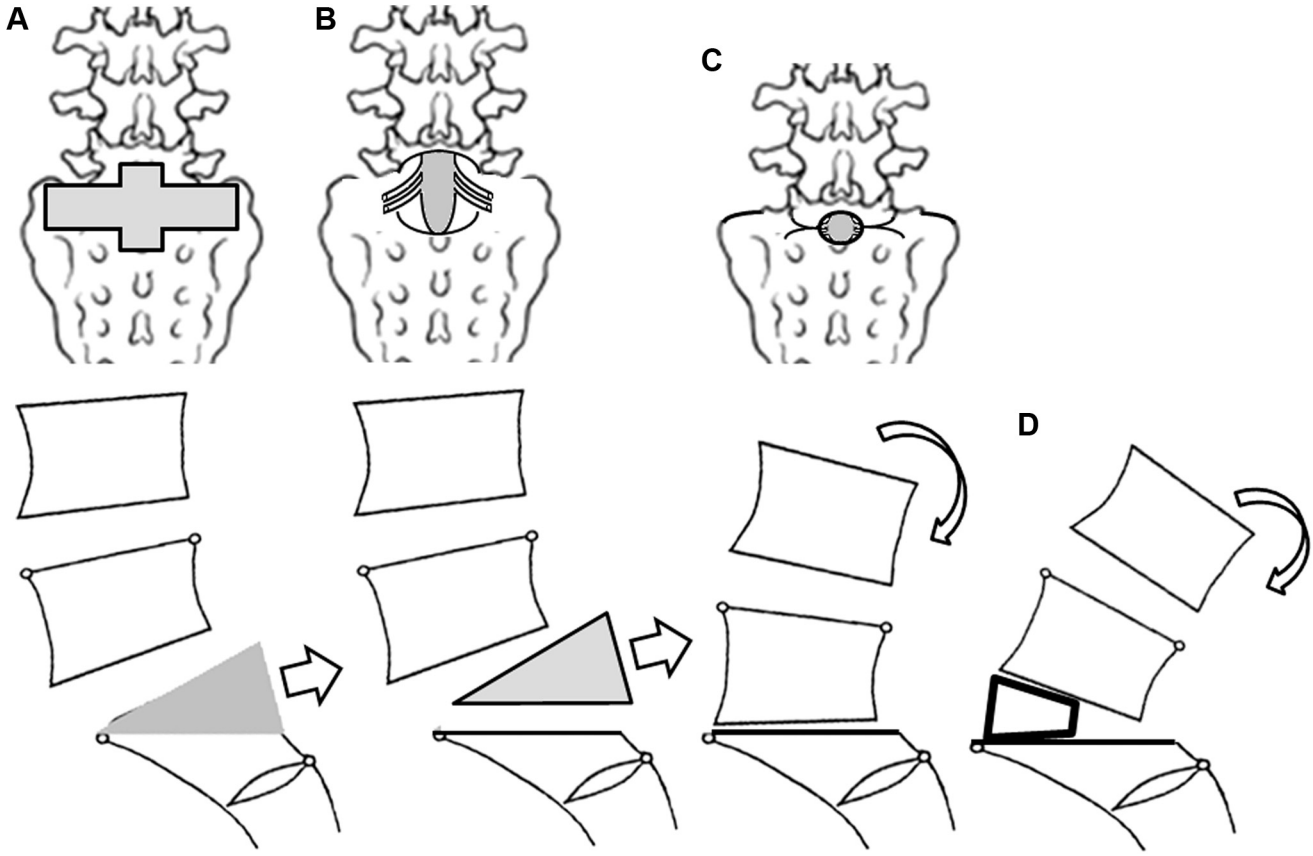

Figure 1. S_1 pedicle subtraction osteotomy (PSO). (**A**) Normal preoperative status with sagittal imbalance; the shaded areas represent the area of bone to be removed. (**B**) S_1 PSO + L_5-S_1 disc removal. Enough posterior decompression is performed to avoid dural buckling or nerve root compression on closing the PSO. (**C**) Closure of the osteotomy with direct bone contact, both anteriorly and laterally, but enough space remains in the posterior area around the thecal sac. (**D**) It is optional to insert an anterior interbody cage after S_1 PSO and L_5-S_1 disc removal to increase the correction.

usually at L_3,[15,38] where it is technically easier, or at L_4.[3] Ten cases have been reported at L_5, 7 had a good clinical result but 3 required an additional surgical procedure.[39] If the technique is performed at L_2, the position of the conus medullaris has to be confirmed preoperatively.[27,38] PSOs are less commonly used in the thoracic spine.[12] The degree of correction can be increased by removing the adjacent disc and inserting an anterior interbody lordotic cage.[37]

Aiming to maximize sagittal spinal imbalance correction, we have devised a PSO variant at S_1 (Figure 1), because for a given angular correction, a more caudally located spinal osteotomy produces a greater overall sagittal balance correction.[3,4,39,40] In addition, any existing spinopelvic imbalances should be corrigible.

Another problem frequently associated with long fixation constructs required for maintaining PSO correction of a spinal deformity is the fracture of the vertebral soma immediately above the last fixed vertebra, known as proximal junctional kyphosis (PJK).[2,14] The longer the fixation construct, the higher the chance that this complication will occur,[17,41] making practical shorter instrumentations desirable.[31] Minimally invasive approaches have been applied in clinical practice[42] but the results have not been encouraging because the degree of correction is limited and reoperations are common.[35] Aiming to reduce the length of the fixation construct, 5 different possibilities of lumboiliac fixation for S_1 PSO were devised in this study.

After an exhaustive bibliographic search, no references to S_1 PSO were found, so a study of human cadaveric specimens was performed to assess the feasibility, requirements, and degree of correction that can be achieved. The hypothesis of this study was that an S_1 PSO allows adequate correction of the sagittal balance, given that being at the base of the spine, smaller osteotomy angles correlate to greater angles of correction at higher levels. The main objective of this study was to biomechanically evaluate the behavior of this S_1 PSO. In addition, 5 different possibilities to achieve a short fusion in this S_1 PSO variant were investigated.

METHODS

Twelve fresh cadavers were provided by the Facultat de Medicina i Odontologia of the the Universitat de Valencia. The cadaveric specimens were kept in a refrigerator from the moment of death until the next morning. The medical records were thoroughly reviewed to exclude specimens with any previous surgical procedures, trauma, malignancy, or disease involving the spine. All contributors had to be older than 18 years. Plain spine anteroposterior and lateral radiographic studies were performed on all the cadavers to rule out any disease, unless recent premorbid spine radiographic examinations were available. Dual energy X-ray absorptiometry scans of the lumbar spine of each specimen were obtained to rule out osteoporosis. Subsequently, all soft tissues were removed except those valuable in biomechanical studies: bone, intervertebral discs, and ligaments. The specimens' spines were sectioned at T_{10}, keeping the last 2 dorsal vertebrae, the lumbar spine, the pelvis, and the upper third of the femur. Each specimen was assigned a number for identification during the study.

Baseline Multislice Computed Tomography Study

It was performed after soft tissue removal, with 0.625-mm section images from T_{10} to the coccyx (GE Healthcare, Milwaukee, Wisconsin, USA). The images were three-dimensionally (3D) reconstructed with a matrix 512×512 and an isotropic voxel of 1×1×1mm. The computed tomography (CT) images were transferred to a computer as DICOM (Digital Imaging and Communications in Medicine). Demineralization was an exclusion criterion, so bone mineral density was assessed.

In each specimen the pelvic incidence (PI), pelvic tilt (PT), sacral slope (SS), and lumbar lordosis (LL) (Figure 2), as described by Lafage et al.,[44] were calculated with a specific software (Materialise Mimics 2017). The iliac screw entry point in the posterosuperior iliac spine (PSIS) and its maximal possible length inserted in the direction of the anterosuperior iliac spine were calculated. Other parameters such as the sagittal vertical axis, the T_1-pelvic angle, or the global tilt, which are proposed by some as more accurate,[45] could not be evaluated because that would require biomechanical studies of the whole spine, which was unfeasible in our laboratory.

Specimens were kept frozen at −25° C until the preoperative biomechanical study, when they were thawed at room temperature for 4–5 hours.

Baseline Biomechanical Study

All the biomechanical studies were performed at 22°C–23°C and 40% humidity. Sodium chloride solution 0.9% was sprayed on

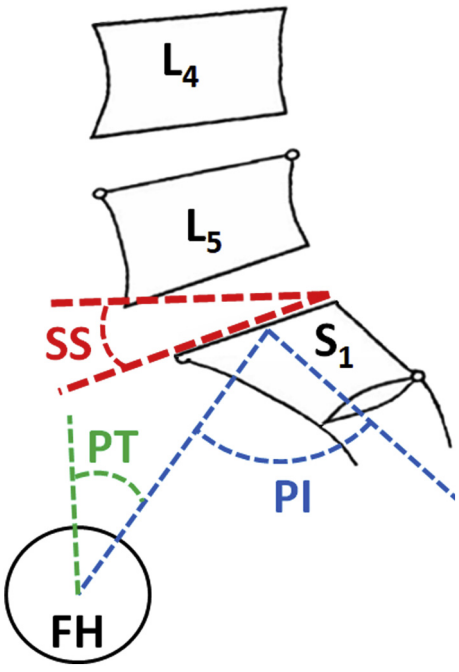

Figure 2. Definitions of the specimen parameters (sacral slope [SS], pelvic tilt [PT], pelvic incidence [PI] and lumbar lordosis) modified from the definitions stated by Garbossa et al.[43] FH, femoral head.

the samples every 5 minutes to prevent tissue desiccation.[46] A polyethylene piece with a semi-spherical seat was screwed onto the superior T_{10} end plate. Both ischia were potted with acrylic bone cement (SR Triplex Cold [Ivoclar Vivadent AG, FL-9494, Schaan, Liechtenstein]), making sure that the disc center plane at L_3 remained horizontal. The symphysis pubis, sacrum, and sacroiliac joints were kept out of the acrylic bone cement.

For the baseline biomechanical study, each specimen was attached to the actuator of the testing machine (INSTRON 8874/135 [Instron Worldwide, Norwood, Massachusetts, USA]). The forces were transmitted through a sphere connected to the actuator, which lodged itself inside the center of the polyethylene piece (Figure 3).

As soon as the preparation was complete, nondestructive biomechanical baseline tests were carried out on the intact specimens to determine the initial stability. Loads of 500 N were applied through a displacement of the actuator in flexion-extension, lateral bending, and axial rotation of 0.03 mm/second. Five identical loading ramps were applied, reaching 500 N each time. The rigidity of the specimen was determined using the last measurement.

Once the biomechanical studies were completed, the specimens were stored at −25°C to prevent decay.

Surgical Procedure: S_1 PSO

The steps for this procedure can be seen in Figure 1. First, specimens were thawed at room temperature for 4–5 hours. Then, the amount of S_1 bone to be removed was evaluated with Surgimap v2.2.11.1 (Nemaris Inc., New York, New York, USA), which included the L_5 spinous process, distal half of L_5 lamina, L_5-S_1 facet joints, S_1 and S_2 posterior arches, both S_1 pedicles, and a wedge-shaped portion of the S_1 vertebral body and sacral alae (Figure 4A). A bone scalpel was used to section the bone (Misonix, Farmingdale, New York, New York, USA), minimizing the dangers related with the use of an osteotome. Bone fragments were carefully removed with bone rongeurs. The thecal sac was moved medially, to allow removal of the posterior wall of the S_1 vertebral body (Figure 4B). A wedge section of the PSIS was removed to prevent the collision of the L_5 pedicle and iliac screws on closing the PSO.

Several components were inserted at this point: multiaxial titanium (Ti6Al4V ELI) pedicle L_4 (6.5×40–50 mm) and L_5 (6.5×40–50 mm) and iliac screws (7.5×70 mm) and rods (diameter 5.50 mm) (Zodiac [Alphatec Spine, Carlsbad, California, USA]) (Figure 4D). Offset connectors were used as required to connect any necessary second iliac screw on the same side.

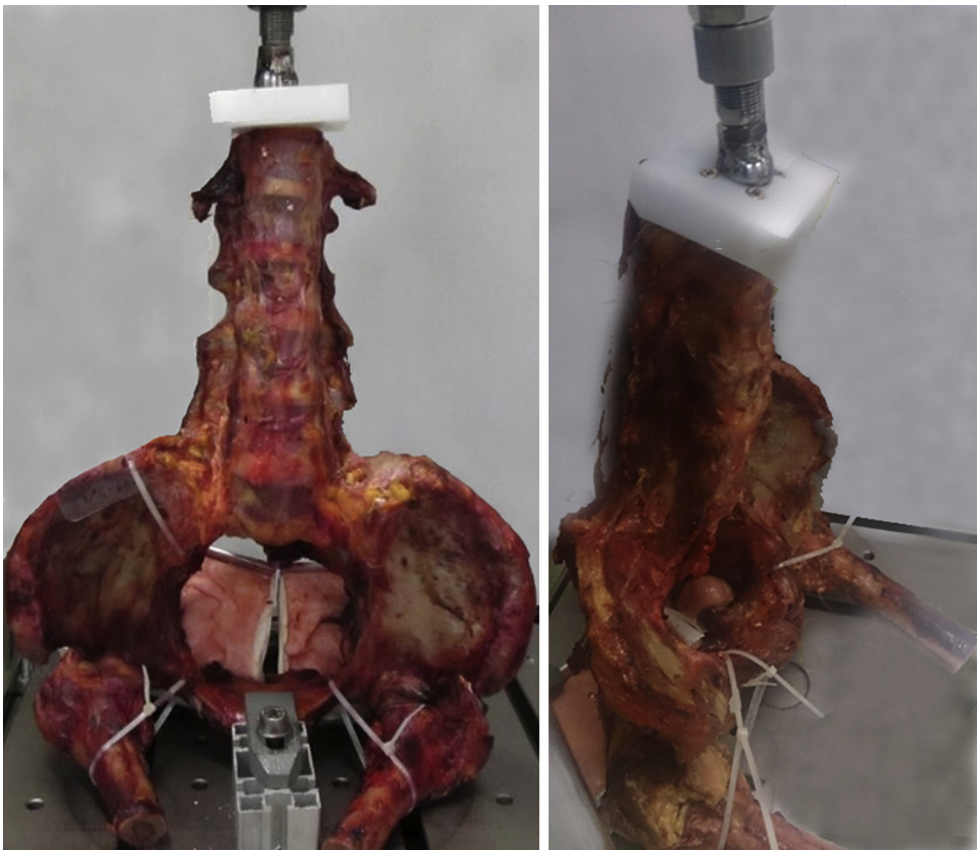

Figure 3. Specimen placed in the testing machine (INSTRON 8874/135 [Instron Worldwide, Norwood, Massachusetts, USA]).

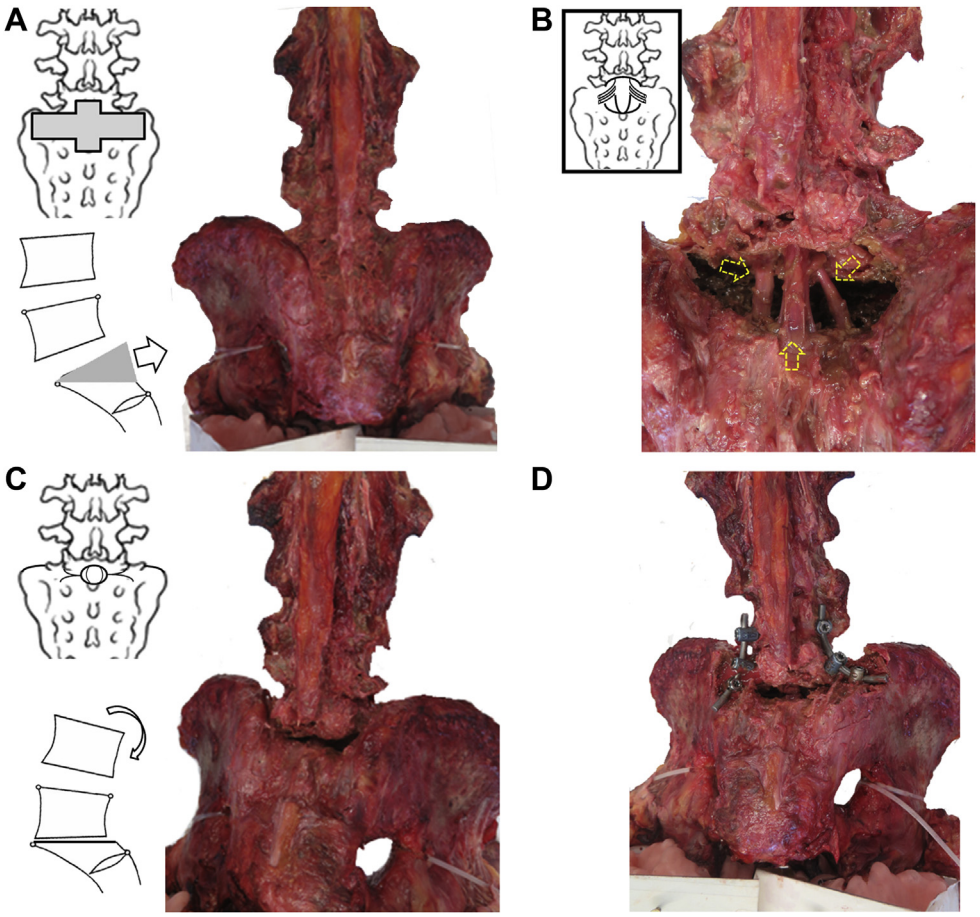

Figure 4. (**A**) Preoperative status of the dorsolumbopelvic specimen. The shading shows the areas of bone to be removed. (**B**) Bone removal completed. The 2 side arrows point to the S1 nerve roots and the lower arrow to the thecal sac. (**C**) The S_1 pedicle subtraction osteotomy is closed, extending the lumbar spine and retroflexing the pelvis. (**D**) Osteotomy closed and stabilized with pedicle and iliac screws connected with titanium bars.

These metal implants were provided by PRIM, S.A. (Mostoles, Madrid, Spain). The iliac screws were inserted through the PSIS. The osteotomy defect was closed, extending the lumbar spine and retroflexing the pelvis (Figure 4C). The thecal sac and the L_5 and S_1 roots were revised to ascertain the absence of any buckling or compressing point. Figure 5 shows one of the specimens before and after the surgical procedure, and the degree of spinal correction.

Post S_1 PSO CT Study

Just after the S_1 PSO was completed, another CT scan was performed to ascertain the amount of bone removal, the changes in the spinopelvic parameters (SS, PI, PT, and LL), and the degree of spinal correction.

Post S_1 PSO Biomechanical Study

Subsequently, the specimens underwent a new biomechanical study, applying the compression loads in the same way and conditions as in the baseline studies. The test was complete after a 500N loading or when a change in the behavior of the specimen was observed visually. The compression stiffness results were determined with equation 1.

$$\text{Compression stiffness} = 500\ \text{N}/\text{maximum displacement under compression(mm)} \quad (1)$$

The stiffness of each instrumented specimen was normalized with its own intact condition (equation 2).

$$\text{Normalized stiffness} = (\text{Post} - \text{surgical stiffness}/\text{Pre} - \text{surgical stiffness}) \times 100 \quad (2)$$

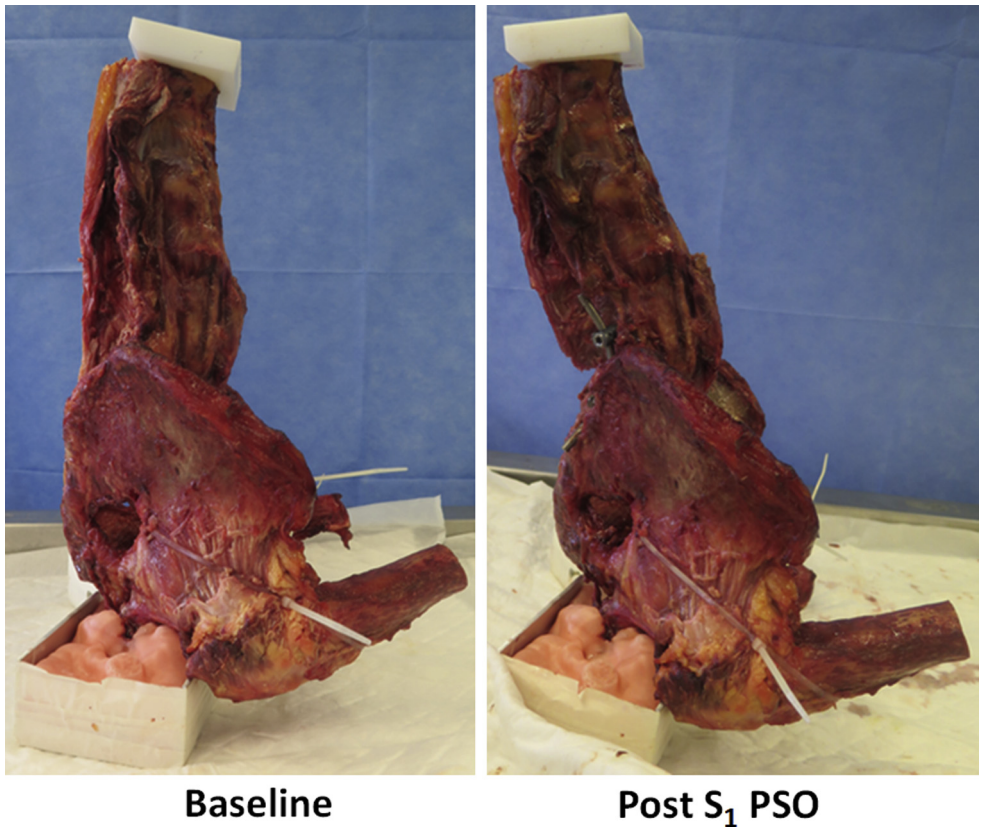

Figure 5. Preoperative (*left*) and postoperative (*right*) images of one of the specimens. PSO, pedicle subtraction osteotomy.

CT Calculation of Sagittal Balance Correction Achieved

Presurgical and postsurgical CT images were compared analyzing the spinal correction achieved. The CT images were transferred into a two-dimensional computer-aided design format using the software MATERIALISE MIMICS 2017 (Materialise, Leuven, Belgium). The data obtained for each specimen from L_4, L_5, sacrum, and iliac parameters were compared between specimens and with those available in the literature. The angle in the sagittal plane between the L_5 and iliac screw tulips was also evaluated.

A PubMed literature search was carried out to find reported correction degrees achieved with a PSO at other levels, the mean height and width values of the lumbar, sacral, and iliac bones, and the forces acting on the sacral region, as well as to confirm that no specimen harbored any atypical bony morphology or spinal angular value and to obtain force values to be able to redesign the metallic implant.

The parameters of our specimens were compared and found to be in concordance with those observed in the literature.

Search for Other Possibilities to Increase the Rigidity of the Fixation Construct

Four additional possibilities were evaluated. First, a 12-mm-high interbody cage was inserted from a posterior approach in the created S_1 osteotomy defect. Then, a cross-connecting bar was placed. The next step was to insert a second iliac screw on each side, connecting it with an affixation bar. An anterior lumbar interbody fusion (ALIF) cage was inserted at the L_5-S_1 disc. After each step, biomechanical studies were performed to find out how much the rigidity of the fixation construct had changed.

Implant Redesign

On attempting to close the S_1 PSO, the L_5 pedicle and iliac crest screws lay adjacent, often colliding with each other. The iliac screw tulip and all its subcomponents (i.e., saddle and locking cap) had to be redesigned because their function was compromised.

Stress and Bending Moment Calculations with the Raw Design of the New Implant

Figure 6 shows a simplified model of the fixation construct. The metal implants were inserted on both sides of the spine. Only the screw 3 tulip (iliac screw) was redesigned. Two specific areas (z1 and z2) were determined as critical, because they are high-risk failure sites. Inertia and stress calculations were performed to ascertain that the implant would not fail under

physiologic loads or under repetitive loading over long periods. These stresses were calculated with the following equations[47,48]:

- Equation 3: inertia calculus

$$I = \pi(2 \times r)^4/64 \quad (3)$$

where I = inertia (m^4) and r = radius of rod and implant's core (m)

- Equation 4: flexor-extensor bending moment calculus

$$M = d \times F \quad (4)$$

where M = flexor-extensor bending moment (N m), d = length of the core of the crewed portion of the implant (m) and F = force (N)

- Equation 5: stress calculus

$$\sigma = F/A \pm (M/I) \times r \quad (5)$$

where σ = stress (N/m^2), F = force (N), A = area (m^2), m = flexor-extensor bending moment (N m) and I = inertia (m^4).

Some considerations were taken into account while carrying out these calculations. The transmitted loads were established as though they passed through an imaginary line that connected the tips of the screws. It was also considered that the vertebrae would not transmit any load; instead, loads would be completely transmitted through the rods. The calculations did not depend on vertebral morphology but on the fixation construct itself.

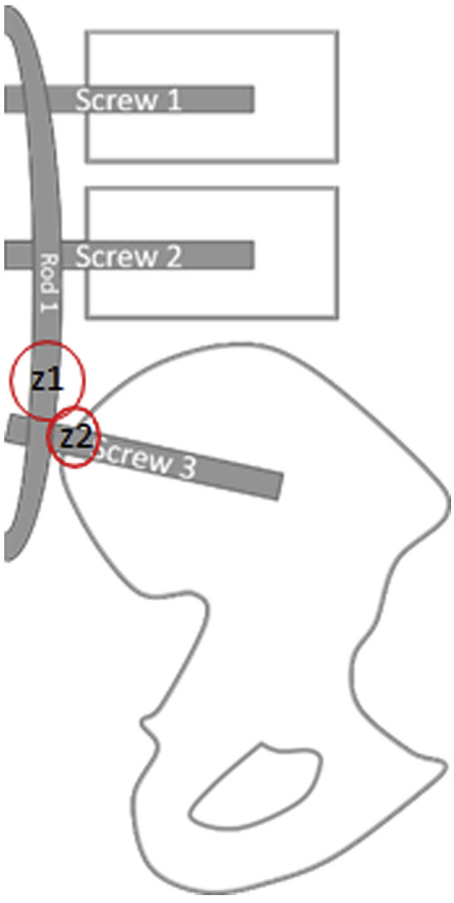

Figure 6. Simplified diagram of one of the fixation construct to be redesigned.

3D Computed Redesign of the Implant Constructs

The tulip of the iliac screw and its subcomponents (saddle and locking cap) were redesigned with the aid of the Design Optimization Software SOLIDWORKS 2015 (Dassault Systems, Vélizy, Villacublay Cedex, France). The L_4 and L_5 pedicle screws did not require any redesign.

Validation of the Redesigned Implant Constructs

This validation was achieved with finite element analysis (FEA) with ANSYS Workbench Student 14.5. software (Ansys Inc., Canonsburg, Pennsylvania, USA). This FEA analysis followed the ASTM F1717–15 Standard Test Methods for Spinal Implant Constructs in a Vertebrectomy Model directive.[49] After importing the computed model of the fixation construct into the ANSYS Workbench, the properties of the new fixation construct material were established. Only Titanium (Ti-6Al-4V ELI) was applied to the model.[50] A mesh was generated using the patch conforming method: the meshing process of a 3D object involves dividing the object into a discrete number of elements, so that when a load is applied, it distributes itself uniformly. The mesh was composed of 1,853,430 nodes and 1,187,904 triangular elements, allowing the geometry to be resolved adequately. The standard gradient analysis indicated that the model could be considered valid.

The external force applied to the fixation construct was set to 400 N based on estimates found in the literature.[51] This setting corresponds to the forces applied to the L_5-S_1 region in humans when standing up straight. Furthermore, the iliac screw head was established as being fixed, whereas the 400-N forces were divided evenly between the L_4 and L_5 pedicle screws (200 N at L_4 and 200 N at L_5) and applied at the head and threaded portion of the pedicle screws. This distribution corresponds to the F1717-15 regulation.[49]

Statistical Analysis

Demographic, radiologic, surgical, and biomechanical data were analyzed using descriptive statistics, performed using both Excel (Microsoft Corporation, Redmond, Washington, USA) and R (R Foundation for Statistical Computing, Vienna, Austria).[52,53] Baseline and postoperative data were compared with the t test, using $P > 0.05$ and a confidence interval of 95% as statistically significant.

RESULTS

Biometric Studies of the Specimens

Only specimens with nonspinal diseases were included in this study. There were 6 men and 6 women, with a mean age of 65.08

Table 1. Baseline L_4 and L_5 Specimen Parameter Statistics

	L4 Vertebral Body Height	L4 Vertebral Body Width	L4 Vertebral Body Depth	L4 Spinal Canal Diameter	L4-I5 Disc Height	L5 Vertebral Body Height	L5 Vertebral Body Width	L5 Vertebral Body Depth	L5 Spinal Canal Diameter	L5-S1 Disc Height
N valid	12	12	12	12	12	12	12	12	12	12
Mean	25.40	46.35	35.15	29.11	13.47	21.40	52.25	34.23	36.00	11.70
Standard deviation	1.23	3.05	2.15	8.65	2.27	2.47	4.21	1.99	2.10	2.37
Range	4.16	10.36	6.40	24.90	7.42	9.32	13.28	6.57	7.27	7.06
Minimum	23.07	40.79	32.02	10.31	8.72	16.71	43.19	30.68	31.87	8.81
Maximum	27.23	51.15	38.42	35.21	16.14	26.03	56.47	37.25	39.14	15.87

Values are in millimeters.

years ± 5.24 standard deviation (SD) (range, 57–73 years). The mean height was 1.71 m ± 0.76 SD (range, 1.59–1.82 m). The mean body weight was 75.08 kg ± 9.68 SD (range, 59–89 kg). The mean body mass index (calculated as weight in kilograms divided by the square of height in meters) was 25.36 ± 1.87 SD (range, 22.66–27.53).

None of the 12 specimens showed signs of mineral decalcification on the CT studies.

Table 1 shows the specimens' L_4 and L_5 dimensions with their statistical analysis. These data were within normal range and comparable to those available in the literature.[9,45,54]

Baseline and postsurgical spinopelvic and LL values are shown in Table 2. Postoperatively, the SS decreases from 35.77° ± 4.82° SD (range, 27.27°–41.37°) to 21.05° ± 3.68° SD (range, 11.05°–23.75°), the PT increases from 12.24° ± 3.08° SD (range, 11.64°–5.89°) to 15.54° ± 3.39° SD (range, 19.92°–9.25°), the PI decreases from 51.70° ± 2.06° SD (range, 48.17°–54.81°) to 35.59° ± 4.51° SD (range, 29.66°–41.17°) and the LL increases from 50.90° ± 7.05° SD (range, 41.36°–60.35°) to 66.84° ± 7.41° SD (range, 55.01°–76.74°). After S_1 PSO, the PI shows the greatest correction (16.11°), followed by LL (15.94°), SS (14.72°), and PT (3.3°) (Table 2). The changes in postoperative LL are difficult to evaluate because the studies were performed lying and with no weight bearing. Nevertheless, the difference in our specimens between the postoperative PI and LL are minimal (0.17°).

Biomechanical Study Results

Stiffness showed a reduction, from 107.17 ± 29.42 N/mm at baseline to 57.94 ± 11.87 N/mm postoperatively, with a normalized stiffness reduction of 58.11 ± 14.97 N/mm. Baseline data show a wide variability, which is reduced postsurgically because the behavior is dictated mainly by the fixation construct.

Figure 7 shows for the same specimen the baseline and postsurgical force-displacement curves. On baseline conditions, the specimens behaved linearly because their elastic region was not trespassed. Postsurgically, the behavior was dictated mainly by the performance of the fixation construct, which was lineal under 500-N loading conditions. The instrumented S_1 PSO had a lower strength than did the intact specimen, and consequently, other possibilities had to be explored, such as adding an interbody cage at the S_1 osteotomy site, a crossbar, 2 iliac screws per side, and an anteriorly inserted L_5-S_1 ALIF cage. All these measures improved similarly the resistance of the fixation construct compared with the S_1 PSO model, but rigidity was still lower than in the intact specimen.

Table 2. Baseline and Postsurgical Results of the Specimen's Spinopelvic and Lumbar Lordosis Parameter Statistics

	SS Baseline	SS Postoperative	PT Baseline	PT Postoperative	PI Baseline	PI Postoperative	LL Baseline	LL Postoperative
N valid	12	12	12	12	12	12	12	12
Mean	35.77	21.05	12.24	15.54	51.70	35.59	50.90	66.84
Standard deviation	4.82	3.68	3.08	3.39	2.06	4.51	7.05	7.41
Range	14.10	12.70	11.64	10.67	6.64	11.51	18.99	21.73
Minimum	27.27	11.05	5.89	9.25	48.17	29.66	41.36	55.01
Maximum	41.37	23.75	17.53	19.92	54.81	41.17	60.35	76.74

Values are grades of angulation.

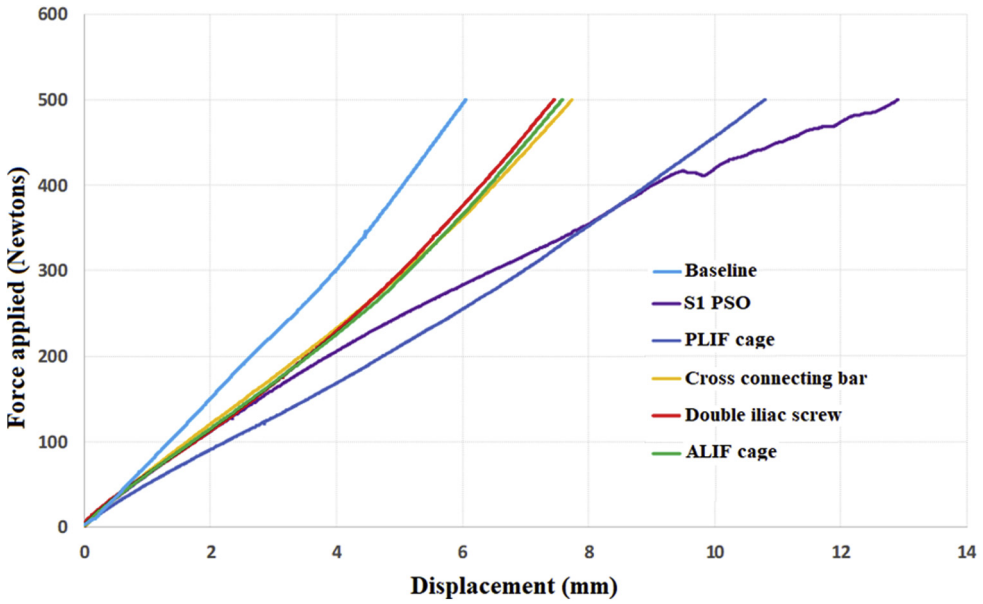

Figure 7. Specimen baseline (intact specimen) and postsurgical force-displacement curves with the S_1 pedicle subtraction osteotomy (PSO) and with the different fixation construct possibilities. ALIF, anterior lumbar interbody fusion; PLIF, posterior lumbar interbody fusion.

Stress Calculations

The construct maximum and minimum stresses of the fusion on applying 400 N can be seen in Table 3. Flexion forces are calculated for the worst-case scenario, where 100 N is applied on the head of the L_4 and L_5 screws and 200 N on the iliac screw and rod. As shown in Figure 6, the iliac screw supports the maximum stress forces, so a second iliac screw improves the rigidity of the fixation construct (Figure 7). In addition, a cross-connecting bar creates a whole unit with the fixation construct from both sides, increasing the construct pull-out strength.

RESULTS FROM THE IMPLANT REDESIGN

The iliac tulip rod channel was redesigned because the angle between the tulips of the L_5 and iliac screws was 15°–25°, angulating it 10° and adding to 2 small fins at one of its ends (Figure 8). In addition, this tulip was lengthened 5 mm and 2 complementary fin slots were added at both ends of the rod channel (Figure 9). A semi-sphere was added to the locking cap contact surface to improve its function (Figure 10).

FEA of the Redesigned Fixation Constructs

The fixation construct was simplified for this analysis. The upper screw corresponds to L_4, the middle to L_5, and the lowest to the iliac screw. No spring elements were introduced between the L_4 and L_5 screws to assess the model under the most unfavorable situation. Physiologic loads were applied to the model including a 400-N compression. Each part of the 2 fixation constructs supported 200 N.

On the axial plane, the iliac screw tilted 45° outward from the L_4 and L_5 pedicle screws, whereas the L_4 and L_5 vertebrae were one on top of another. On the sagittal plane, the iliac screw tilted 10° away from the L_4 and L_5 screws. Table 4 shows the mesh properties. The tips of the L_4 and L_5 screws received a 100-N force from above, whereas the iliac screw tip and threaded portion were established as a fixed support. This configuration

Table 3. Stress Calculations of the Different Parts of the System

	Length (m)	Inertia (m^4) ($\times 10^{-12}$)	Flexion Force (N)	Flexor-Extensor Bending Moment (N m)	Maximum Stress (MPa)
L_4 screw	0.04	87.62	100	4	456.52
L_5 screw	0.05	87.62	100	5	570.65
Iliac screw	0.07	155.32	200	14	780.69
Rod	0.1	63.62	200	2	314.44

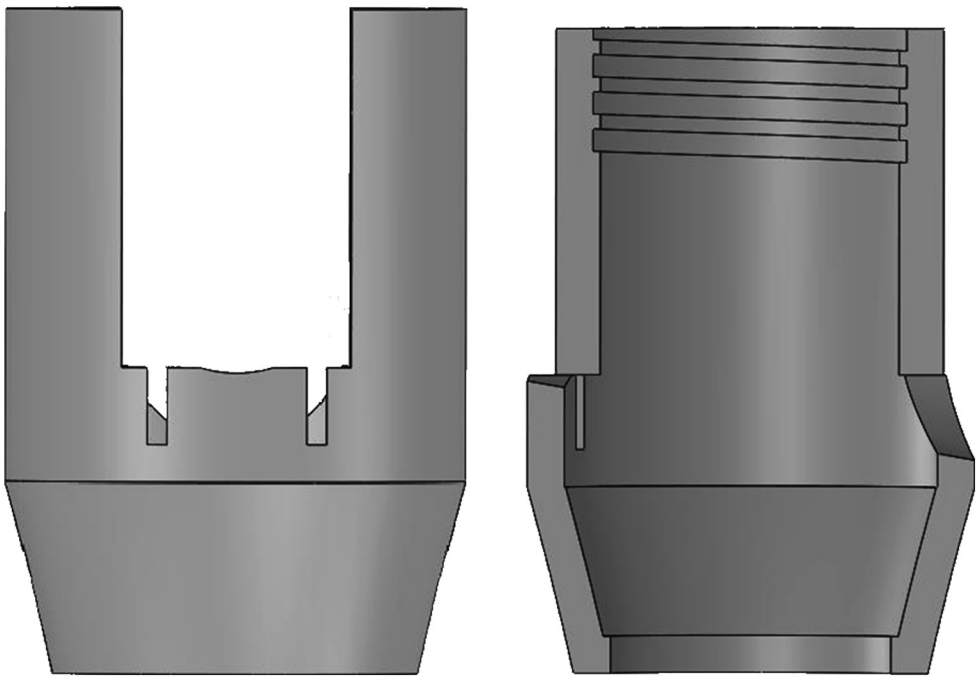

Figure 8. (*Left*) Three-dimensional view of the iliac tulip exterior. (*Right*) Three-dimensional view of the iliac tulip interior.

complies with the F1717-15 regulation,[49] which defines the standard test methods for spinal implant constructs.

The FEA results are shown in Figures 11–14. Figure 11 shows the total deformation. The predicted stresses are low, indicating relatively small local stresses. Therefore, the complete fixation construct is unlikely to fail with loads <400 N. The biggest stresses occur at the meeting point between the iliac screw and its tulip, but the deformations predicted by the model are still within the acceptable range.

Figure 12 shows the equivalent elastic strain generated on the model, the largest being 0.026 mm/mm and located at the topmost portion of the fixation construct. Figure 13 shows that the exact point of these strains was at the boundary between the rod and the iliac tulip.

Figure 14 shows the equivalent von Mises stress predicted by the ANSYS simulation. The biggest stresses predicted by this model were 1.65 GPa, occurring in a small point instead of over a larger area. The z1 and z2 areas received the largest strains, of about 776 MPa, occurring in z1 at the boundary between the rod and the iliac tulip. This is about the same value (780 MPa) predicted in a previous section of our study.

Table 5 indicates the maximum stress values of different components of the construct system. The maximum qualitative values are greater than those predicted by the FEA, although

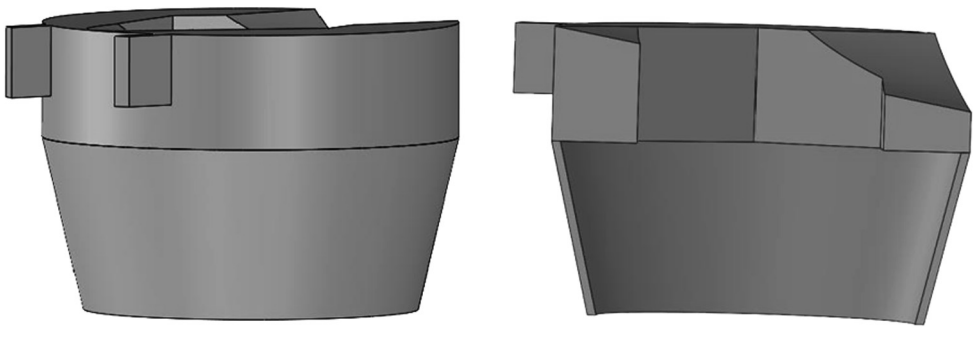

Figure 9. (*Left*) Three-dimensional view of the iliac saddle exterior. (*Right*) Three-dimensional view of the iliac saddle interior.

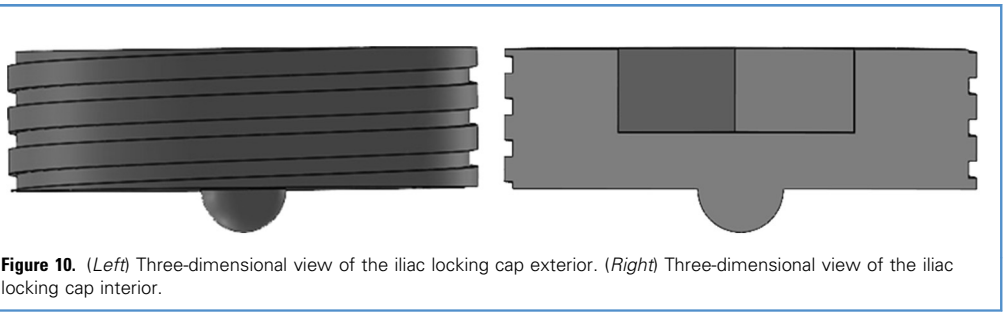

Figure 10. (*Left*) Three-dimensional view of the iliac locking cap exterior. (*Right*) Three-dimensional view of the iliac locking cap interior.

this difference was not statistically significant. Therefore, the model proposed for the stress calculations was correct even although it was a simplification.

DISCUSSION

Baseline spinopelvic and LL parameters of our specimens are comparable to those found in the literature,[9,55] confirming that they were within normal range.

Surgical correction of fixed spinal deformities, particularly those involving sagittal imbalance, requires the use of spinal osteotomies.[31] This strategy entails risky operations aggravated by the fact that most patients are elderly and with comorbidities.[17,31,56] The PSO is the most effective and widely used of these osteotomies.[36,57] It is usually performed at L_3 or L_4 because there is no spinal cord at this level,[31,58] and the more caudal it is performed, the greater the correction.[3,39] Our data show that the PSO at S_1 allows the biggest sagittal balance correction with a single osteotomy, helping to recover it not only by altering the LL but also by adjusting the spinopelvic parameters. In our specimens, the greatest parameter correction in S_1 PSO corresponds to PI (16.11°), followed by LL (15.94°), SS (14.72°), and PT (3.3°). This finding confirms that change in pelvic parameters changes lumbar spine parameters and thus the spinal deformity.

S_1 PSO and SS

The S_1 PSO induces a direct change in the SS at the base of the spine, inducing a sagittal balance modification that has its maximum effect with the same amount of bone resection.[4,10] The spine is moved backward to a more centered position.

S_1 PSO and PI

The PI is related to the normal spine development[59] and is the only spinopelvic parameter that does not change throughout adult life or by compensatory mechanisms.[59] In our specimens, the S_1 PSO modified this parameter, decreasing it by 16.11° and increasing the LL by 15.94°. These data confirm the relationship between PI and LL, as suggested by other investigators.[60,61] In a well-balanced spine, it is estimated that PI = LL $< \pm$ 9°,[11] LL = PI + 10°,[26] or LL = 0.54 × PI + 27.6°.[9] This finding applies to the baseline status of the specimens in this study but not to the postoperative status, confirming that S_1 PSO changes the spinopelvic parameters, whereas PSOs at higher levels do not.

S_1 PSO and PT

PT measures the degree of pelvic retroversion. As its value increases, so does the torque and thus the power needed by muscles to maintain balance.[62] Values >20° reflect an excessive pelvic retroversion, attempting to correct the sagittal imbalance, and correlate with a poor quality of life.[44,62] In our specimens, this parameter increased postoperatively by an average 3.3°, but the final figure (15.54° ± 3.39° SD; range, 19.92°–9.25°) remained inside the safe zone.

S_1 PSO and Fusion Construct Length

Long spine fusions eliminate some of the natural mechanisms to recover the spinal balance, reducing the patient's "cone of economy."[17] A more rigid spine may not necessarily correlate with a better spinal balance.[17] Some have suggested that moving the PSO caudally would reduce the number of levels that need to be fixed as well as the chance of instrumentation failure and pseudoarthrosis.[4] This study shows that S_1 PSO leads to a better correction of the sagittal balance with a shorter fusion. Five different fixation constructs were also investigated to distinguish any differences among them, finding that a bilateral posterolateral L_4-L_5-iliac fusion with a polyetheretherketone (PEEK) cage and a crossbar provides satisfactory rigidity. A double iliac screw per side also increases stability but further additions to the fixation construct do not significantly improve the results. S_2 alar-iliac (S_2AI) screws could be an interesting alternative to iliac screws but were not explored in this study.

Implant Failure in PSO

PSO implant failure affects 22% of cases,[63] with an incidence higher at L_4 than at L_3.[43,64,65] No conclusions can be drawn at L5 because only 10 PSO cases have been reported.[39] The risk of PSO implant failure can be reduced by inserting interbody cages at the PSO,[66,67] using cobalt-chrome[39,57,64] instead of stainless steel or titanium implants[43,63] or inserting a double rod.[39,43,64,68-71] Titanium has the advantage that it is compatible with postoperative magnetic resonance imaging and the disadvantages of microfracture propagation and being notch-sensitive after intraoperative contouring.[72] The rod diameter is also important because 6-mm rods are stronger and fail less often, particularly if they are made out of cobalt-chrome.[43,71] Rod fracture has been estimated to affect 6.9% of lumbar PSOs.[15,63] In this study, titanium implants were used to increase the feasibility of postoperative imaging studies and because the long-term durability of these fixation constructs was not relevant, because no long-term biomechanical studies were to

Table 4. Mesh Properties

Object Name	Mesh
State	Solved
Defaults	
Physics preference	Mechanical
Relevance	0
Sizing	
Use advanced size function	On: proximity and curvature
Relevance center	Medium
Initial size seed	Active assembly
Smoothing	Medium
Transition	Fast
Span angle center	Medium
Curvature normal angle	Default (45.0°)
Proximity accuracy	0.5
Num cells across gap	Default (3)
Minimum size	Default (3.5394e−002 mm)
Proximity minimum size	Default (3.5394e−002 mm)
Maximum face size	Default (3.53940 mm)
Maximum size	Default (7.07890 mm)
Growth rate	Default (1.850)
Minimum edge length	3.1416e−004 mm
Inflation	
Use automatic inflation	None
Inflation option	Smooth transition
Transition ratio	0.272
Maximum layers	5
Growth rate	1.2
Inflation algorithm	Pre
View advanced options	No
Patch conforming options	
Triangle surface mesher	Program controlled
Advanced	
Shape checking	Standard mechanical
Element midside nodes	Program controlled
Straight-sided elements	No
Number of retries	0
Extra retries for assembly	Yes
Rigid body behavior	Dimensionally reduced
Mesh morphing	Disabled
Defeaturing	
Pinch tolerance	Default (3.1855e−002 mm)
Generate pinch on refresh	No
Automatic mesh-based defeaturing	On
Defeaturing tolerance	Default (1.7697e-002 mm)
Statistics	
Nodes	1,853,430
Elements	1,187,904
Mesh metric	None

Continues

be performed. Further studies are required to confirm which materials or number of rods can reduce implant failure rate with S_1 PSO.

S_1 PSO and Fusion Construct Stiffness

In this study, the average postoperative S_1 PSO stiffness decreased 56.4 N/mm below the baseline, which was corrected using an L_5-S_1 interbody PEEK cage (as recommended in PSO at higher levels),[57,66,67,73] a second iliac screw on either side,[74] and a cross-connecting bar.[15,71,75-77] The L_5-S_1 PEEK cage reduces the rod stress by 15%[68] and the chance of pseudoarthrosis.[15,66,69,75,78] The ALIF cage had the maximum effectivity[26,75,79] but in real life, it would involve a second surgical approach, reducing its applicability in clinical practice. Nevertheless, the interbody cage acts by maintaining the disc height although its contribution to spine stability after osteotomy is limited.[75] Its main effect is to prevent the anterior

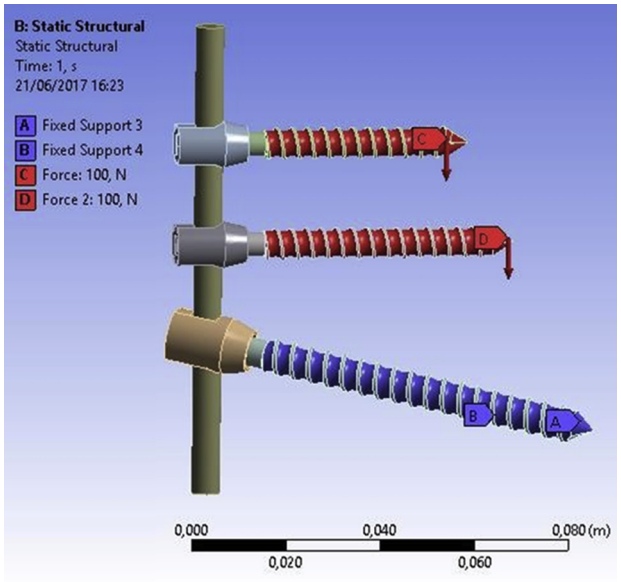

Figure 11. Boundary conditions applied onto the model.

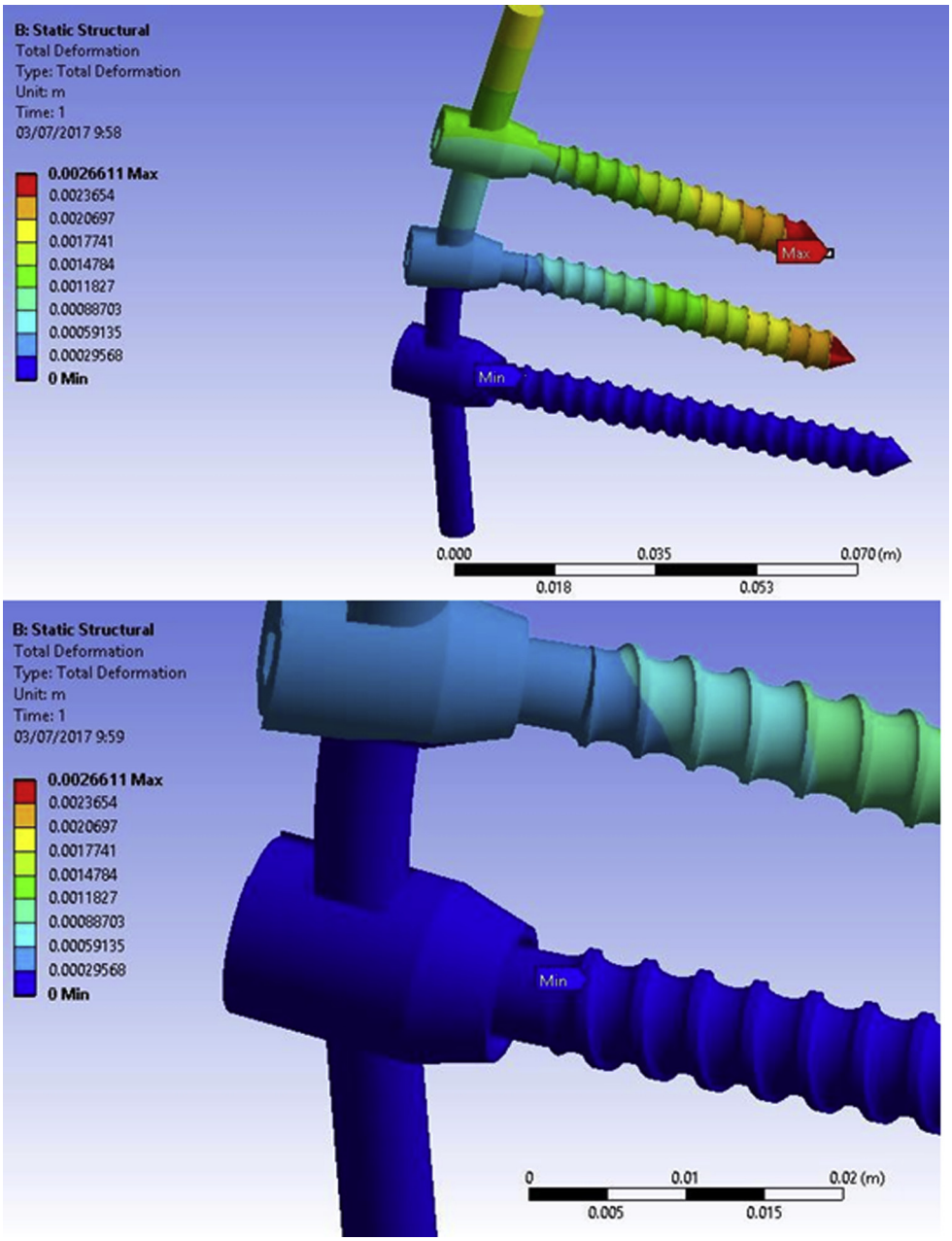

Figure 12. (*Top*) Total deformation in the construct. (*Bottom*) Close-up total deformation of the z1 and z2 areas of the fixation construct.

collapse of the construct, because this increases significantly the forces that the posterior fixation equipment has to stand.[75] The S_2AI provides 14 N m/degree of additional improvement in spinopelvic fixation[46] and it is as strong as the iliac screw but without the dangers of increased tissue handling and prominence with risk of skin ulceration.[46,77] In any case, the use of this S_2AI was not attempted in this study. Two rods per side reduced the stress of the primary rod by 51%[68] but rigid fixation constructs are not desirable because the load at the osteotomy site is necessary to induce new bone creation with callus formation.[43] The most frequent place for rod fracture is at the point of maximum bending,[63,75,80] particularly with the titanium rods and less with the cobalt-chrome rods.[43,68] Thus, the use of precontoured rods has been strongly recommended.[43,64] With the addition of a second rod per side, it is recommended to place it as posteriorly as possible, because this

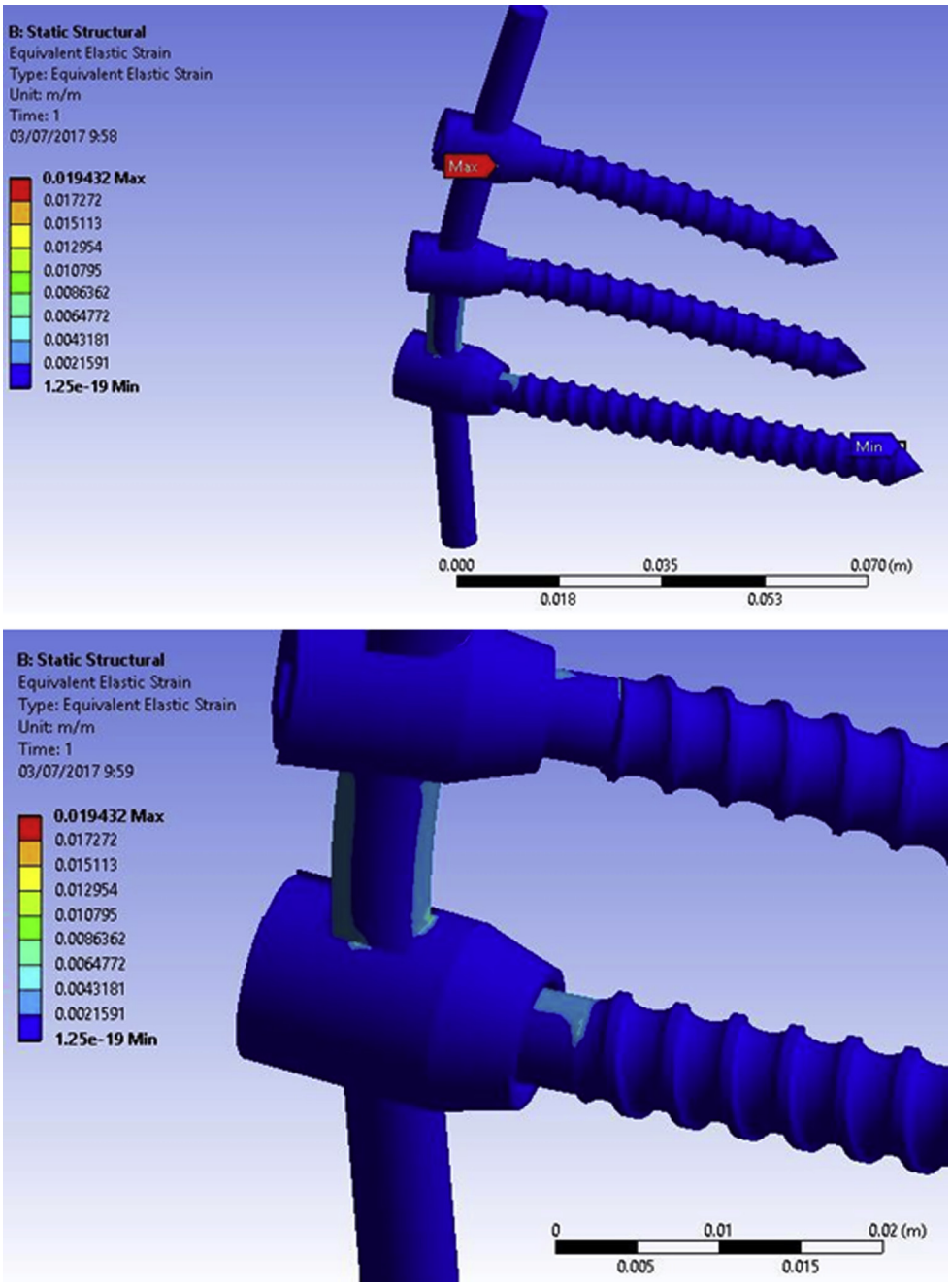

Figure 13. (*Top*) Equivalent elastic strain in the construct. (*Bottom*) Close-up equivalent elastic strain deformation of the z1 and z2 areas of the fixation construct.

increases the resistance of the fixation construct.[43] More research might be directed toward this possibility in future studies. The S_1 PSO with a bilateral posterolateral L_4-L_5-iliac fusion with a PEEK cage and a crossbar is strong enough in the acute biomechanical test and further additions (dual iliac screw and ALIF cage) are not needed, as shown in this study.

S_1 PSO and PJK

PJK is a complication associated with long instrumentation constructs,[2,14] with an incidence proportional to the length of the fusion.[17,41] It is frequent with PSO at L_3[81] or L_4,[82] making it advisable to search for shorter fixation constructs capable of maintaining the spinal deformity correction.[31] Minimally invasive

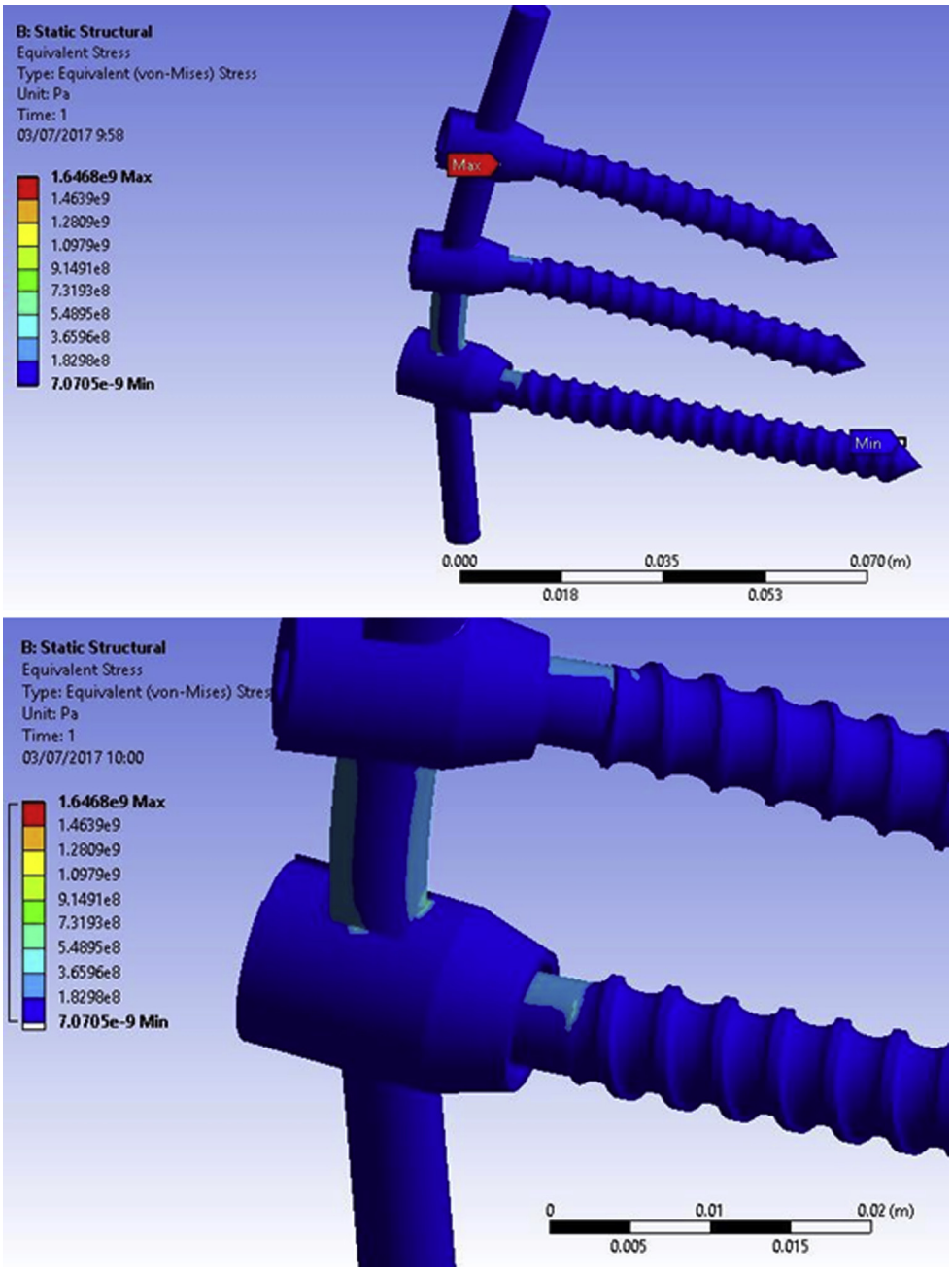

Figure 14. (*Top*) Equivalent (von Mises) stress in the construct. (*Bottom*) Close-up equivalent (von Mises) stress of the z1 and z2 areas of the fixation construct.

approaches have been introduced to reduce the length of the fixation constructs,[33,42] but the deformity correction is limited and the reoperation rate is high.[35,42,83] It has been reported that a 2-level fixation above and below a PSO with an interbody cage provides enough rigidity to the fixation construct.[64] In this way, the S_1 PSO short fixation construct should reduce the incidence of PJK, but there are no long-term biomechanical data. Another consideration to avoid this complication is that the rods should not extend past the tulips at the upper fused level.[39]

S_1 PSO and Redesign Iliac Screw Tulip

The existing fixation constructs are difficult to mount in the S_1 PSO, because the L_5 pedicle and iliac screws lie closer together than in PSO at higher spinal levels. After thorough revision of

Table 5. Maximum Stress Values of the Different Fusion Construct Components

	Maximum Qualitative Stress (MPa)	Maximum Finite Element Analysis Stress (MPa)
L_4 screw	456.52	453.18
L_5 screw	570.65	575.63
Iliac screw	780.69	776.02
Rod	314.44	325.66

the available fixation systems, we selected the Zodiac Degenerative—Spinal Fixation System (Alphatech Spine, Carlsbad, California, USA). The iliac screw tulip and its subcomponents (saddle and locking cap) were redesigned to reduce the drawbacks derived from the fact that on closing the S_1 PSO, the L_5 and iliac screws collided with each other. Its rod channel was angulated 10°, and a semi-sphere to the locking cap contact surface and 2 fins at its saddle were added. According to our FEA studies, this redesigned tulip should tolerate loads up to 400 N, show excellent biomechanical properties, and adapt to the specific S_1 PSO requirements. It has not been clinically tested yet but our data strongly suggest that it would adapt to its intended use.

Limitations

Limitations of this study are that it included cadaveric spine specimens devoid of muscles, that the number of specimens was limited, and that it involved only acute biomechanical tests but no long-term studies. Only the lumbar area was analyzed but not the whole spine, so the sagittal balance could not be assessed. To achieve this goal, CT studies of the whole spine should be taken, or at least from C_7 or T_1 down to the pelvis. This strategy was impractical and would interfere with biomechanical studies. The loads applied to the spinal specimens devoid of live muscle support are a crude approximation to real life. In addition, the fixation of the caudal side of the specimens in a plastic cement construct model might be stiffer than the natural situation in a live human being, and the possible compensation induced by hip and knee flexion was not evaluated. There are no data indicating how much the alternating freezing and thawing of the specimens could have affected their biomechanical properties. This study considered 5 methods of spinopelvic fixation for S_1 PSO, but perhaps other options, such as S_2AI or a double rod, might be even better.

The strength of this study is that each specimen serves as its own control.

CONCLUSIONS

PSO at S_1 is feasible, with a greater degree of correction compared with the same technique at higher levels.

S_1 PSO requires a specifically designed fixation construct, which is not available in the market.

The following innovations of the iliac screw tulip are proposed:

1) Angulation of its rod channel by 10°
2) Addition of a semi-sphere to its locking screw contact surface
3) Addition of 2 fins to its saddle at the contact site with the rod.

This new fixation construct model has better biomechanical properties than the commercially available models when used for S_1 PSO and avoids collision between the L_5 and iliac screw tulips. The force calculations and FEA analysis values validate our results.

ACKNOWLEDGMENTS

We thank Juan Gómez, researcher at the Instituto de Biomecánica de Valencia (IBV), Spain, for helping us in using the SolidWorks program to generate the model. We also thank Manolo Montagud (sales representative from PRIM SA, official local distributor of Alpha Tech) for facilitating the implants for this project. We are grateful to the Department of Human Anatomy and Embryology of the Faculty of Medicine of the University of Valencia, particularly to the laboratory curators Lucia and Carmina and to Doctor Tomás Hernández Gil de Tejada and to all personnel of the Instituto de Medicina Legal de Valencia for their assistance in this study.

REFERENCE

1. Glassman SD, Bridwell K, Dimar JR, Horton W, Berven S, Schwab F. The impact of positive sagittal balance in adult spinal deformity. *Spine*. 2005;30:2024-2029.
2. Akbar M, Wiedenhöfer B. [Sagittal deformity. Basic principles of surgical strategies]. *Orthopade*. 2011;40:661-671 [in German].
3. Lafage V, Schwab F, Vira S, et al. Does vertebral level of pedicle subtraction osteotomy correlate with degree of spinopelvic parameter correction? *J Neurosurg Spine*. 2011;14:184-191.
4. Angevine PD, Bridwell KH. Sagittal imbalance. *Neurosurg Clin North Am*. 2006;17:353-363.
5. Le Huec JC, Leijssen P, Duarte M, Aunoble S. Thoracolumbar imbalance analysis for osteotomy planification using a new method: FBI technique. *Eur Spine J*. 2011;20(suppl 5):669-680.
6. Dubousset J. Reflections of an orthopaedic surgeon on patient care and research into the condition of scoliosis. *J Pediatr Orthop*. 2011; 31(1 suppl):S1-S8.
7. Le Huec JC, Saddiki R, Franke J, Rigal J, Aunoble S. Equilibrium of the human body and the gravity line: the basics. *Eur Spine J*. 2011; 20(suppl 5):558-563.
8. Sugrue PA, McClendon J, Smith TR, et al. Redefining global spinal balance: normative values of cranial center of mass from a prospective cohort of asymptomatic individuals. *Spine*. 2013;38: 484-489.
9. Le Huec JC, Hasegawa K. Normative values for the spine shape parameters using 3D standing analysis from a database of 268 asymptomatic Caucasian and Japanese subjects. *Eur Spine J*. 2016; 25:3630-3637.
10. Smith JS, Shaffrey CI, Lafage V, et al. Spontaneous improvement of cervical alignment after correction of global sagittal balance following pedicle subtraction osteotomy. *J Neurosurg Spine*. 2012;17: 300-307.
11. Schwab F, Patel A, Ungar B, Farcy J-P, Lafage V. Adult spinal deformity-postoperative standing imbalance: how much can you tolerate? An overview of key parameters in assessing alignment and planning corrective surgery. *Spine*. 2010;35: 2224-2231.

12. Yang BP, Ondra SL, Chen LA, Jung HS, Koski TR, Salehi SA. Clinical and radiographic outcomes of thoracic and lumbar pedicle subtraction osteotomy for fixed sagittal imbalance. *J Neurosurg Spine*. 2006;5:9-17.

13. Buchowski JM, Bridwell KH, Lenke LG, et al. Neurologic complications of lumbar pedicle subtraction osteotomy: a 10-year assessment. *Spine*. 2007;32:2245-2252.

14. Yagi M, King AB, Cunningham ME, Boachie-Adjei O. Long-term clinical and radiographic outcomes of pedicle subtraction osteotomy for fixed sagittal imbalance: does level of proximal fusion affect the outcome? Minimum 5-year follow-up. *Spine Deform*. 2013;1:123-131.

15. Cho K-J, Kim K-T, Kim W-J, et al. Pedicle subtraction osteotomy in elderly patients with degenerative sagittal imbalance. *Spine*. 2013;38: E1561-E1566.

16. Chang K-W, Leng X, Zhao W, et al. Quality control of reconstructed sagittal balance for sagittal imbalance. *Spine*. 2011;36:E186-E197.

17. Diebo BG, Henry J, Lafage V, Berjano P. Sagittal deformities of the spine: factors influencing the outcomes and complications. *Eur Spine J*. 2015; 24(suppl 1):S3-S15.

18. Geck MJ, Macagno A, Ponte A, Shufflebarger HL. The Ponte procedure: posterior only treatment of Scheuermann's kyphosis using segmental posterior shortening and pedicle screw instrumentation. *J Spinal Disord Tech*. 2007;20:586-593.

19. Ponte A, Orlando G, Siccardi GL. The true Ponte osteotomy: by the one who developed it. *Spine Deform*. 2018;6:2-11.

20. Smith-Petersen MN, Larson CB, Aufranc OE. Osteotomy of the spine for correction of flexion deformity in rheumatoid arthritis. *Clin Orthop*. 1969;66:6-9.

21. Bridwell KH, Lewis SJ, Rinella A, Lenke LG, Baldus C, Blanke K. Pedicle subtraction osteotomy for the treatment of fixed sagittal imbalance. Surgical technique. *J Bone Joint Surg Am*. 2004;86-A(suppl 1):44-50.

22. Boachie-Adjei O, Bradford DS. Vertebral column resection and arthrodesis for complex spinal deformities. *J Spinal Disord*. 1991;4:193-202.

23. Abulizi Y, Liang W-D, Maimaiti M, Sheng W-B. Smith-Petersen osteotomy combined with anterior debridement and allografting for active thoracic and lumbar spinal tuberculosis with kyphotic deformity in young children: A prospective study and literature review. *Medicine (Baltimore)*. 2017;96: e7614.

24. Kim K-T, Park K-J, Lee J-H. Osteotomy of the spine to correct the spinal deformity. *Asian Spine J*. 2009;3:113-123.

25. Bao H, He S, Liu Z, Zhu Z, Qiu Y, Zhu F. Will immediate postoperative imbalance improve in patients with thoracolumbar/lumbar degenerative kyphoscoliosis? A comparison between Smith-Petersen osteotomy and pedicle subtraction osteotomy with an average 4 years of follow-up. *Spine*. 2015;40:E293-E300.

26. Popa I, Oprea M, Andrei D, Mercedesz P, Mardare M, Poenaru DV. Utility of the pedicle subtraction osteotomy for the correction of sagittal spine imbalance. *Int Orthop*. 2016;40: 1219-1225.

27. Qian B, Wang X, Qiu Y, et al. The influence of closing-opening wedge osteotomy on sagittal balance in thoracolumbar kyphosis secondary to ankylosing spondylitis: a comparison with closing wedge osteotomy. *Spine*. 2012;37:1415-1423.

28. Kim YJ, Bridwell KH, Lenke LG, Cheh G, Baldus C. Results of lumbar pedicle subtraction osteotomies for fixed sagittal imbalance: a minimum 5-year follow-up study. *Spine*. 2007;32: 2189-2197.

29. Smith JS, Shaffrey CI, Glassman SD, et al. Risk-benefit assessment of surgery for adult scoliosis: an analysis based on patient age. *Spine*. 2011;36: 817-824.

30. Cho SK, Bridwell KH, Lenke LG, et al. Major complications in revision adult deformity surgery: risk factors and clinical outcomes with 2- to 7-year follow-up. *Spine*. 2012;37:489-500.

31. Heary RF, Kumar S, Bono CM. Decision making in adult deformity. *Neurosurgery*. 2008;63(3 suppl): 69-77.

32. Kim YJ, Hyun S-J, Cheh G, Cho SK, Rhim S-C. Decision making algorithm for adult spinal deformity surgery. *J Korean Neurosurg Soc*. 2016;59: 327-333.

33. Lee C-S, Park S-J, Chung S-S, Lee J-Y, Yum T-H, Shin S-K. Mini-open anterior lumbar interbody fusion combined with lateral lumbar interbody fusion in corrective surgery for adult spinal deformity. *Asian Spine J*. 2016;10:1023-1032.

34. Demirkiran G, Theologis AA, Pekmezci M, Ames C, Deviren V. Adult spinal deformity correction with multi-level anterior column releases: description of a new surgical technique and literature review. *Clin Spine Surg*. 2016;29: 141-149.

35. Hamilton DK, Kanter AS, Bolinger BD, et al. Reoperation rates in minimally invasive, hybrid and open surgical treatment for adult spinal deformity with minimum 2-year follow-up. *Eur Spine J*. 2016;25:2605-2611.

36. Bridwell KH. Decision making regarding Smith-Petersen vs. pedicle subtraction osteotomy vs. vertebral column resection for spinal deformity. *Spine*. 2006;31(19 suppl):S171-S178.

37. Boachie-Adjei O, Ferguson JAI, Pigeon RG, Peskin MR. Transpedicular lumbar wedge resection osteotomy for fixed sagittal imbalance: surgical technique and early results. *Spine*. 2006;31: 485-492.

38. Chen IH, Chien JT, Yu TC. Transpedicular wedge osteotomy for correction of thoracolumbar kyphosis in ankylosing spondylitis: experience with 78 patients. *Spine*. 2001;26:E354-E360.

39. Alzakri A, Boissière L, Cawley DT, et al. L5 pedicle subtraction osteotomy: indication, surgical technique and specificities. *Eur Spine J*. 2018;27: 644-651.

40. van Royen BJ, Scheerder FJ, Jansen E, Smit TH. ASKyphoplan: a program for deformity planning in ankylosing spondylitis. *Eur Spine J*. 2007;16: 1445-1449.

41. Ha Y, Maruo K, Racine L, et al. Proximal junctional kyphosis and clinical outcomes in adult spinal deformity surgery with fusion from the thoracic spine to the sacrum: a comparison of proximal and distal upper instrumented vertebrae. *J Neurosurg Spine*. 2013;19:360-369.

42. Wang MY, Madhavan K. Mini-open pedicle subtraction osteotomy: surgical technique. *World Neurosurg*. 2014;81:843.e11-843.e14.

43. Luca A, Ottardi C, Sasso M, et al. Instrumentation failure following pedicle subtraction osteotomy: the role of rod material, diameter, and multi-rod constructs. *Eur Spine J*. 2017;26:764-770.

44. Lafage V, Schwab F, Patel A, Hawkinson N, Farcy J-P. Pelvic tilt and truncal inclination: two key radiographic parameters in the setting of adults with spinal deformity. *Spine*. 2009;34: E599-606.

45. Banno T, Togawa D, Arima H, et al. The cohort study for the determination of reference values for spinopelvic parameters (T1 pelvic angle and global tilt) in elderly volunteers. *Eur Spine J*. 2016;25: 3687-3693.

46. Burns CB, Dua K, Trasolini NA, Komatsu DE, Barsi JM. Biomechanical comparison of spinopelvic fixation constructs: iliac screw versus S2-alar-iliac screw. *Spine Deform*. 2016;4:10-15.

47. Sánchez C, Del JC. Apuntes para una breve introducción a la Resistencia de Materiales y temas relacionados. 2012. Available at: http://uvadoc.uva.es/handle/10324/2029 [in Spanish]. Accessed May 12, 2017.

48. Anexo_RES_MAT.pdf [Internet]. Available at: https://poliformat.upv.es/access/content/group/DOC_34380_2016/CLASE%203.%20PRESENTACI%C3%93N%20DE%20LOS%20DISE%C3%91OS%203D/Anexo_RES_MAT.pdf, 2016. Accessed May 12, 2017.

49. AENOR: Norma ASTM F1717-15 [Internet]. Available at: http://www.aenor.es/aenor/normas/astm/fichanormaastm.asp?codigo=091661#.WOdTz9LhA2w. Accessed August 8, 2018.

50. Sterling A, Shamsaei N, Torries B, Thompson SM. Data related to cyclic deformation and fatigue behavior of direct laser deposited Ti-6Al-4V with and without heat treatment. *Data Brief*. 2016;6: 970-973.

51. Kiapour A, Abdelgawad AA, Goel VK, Souccar A, Terai T, Ebraheim NA. Relationship between limb length discrepancy and load distribution across the sacroiliac joint—a finite element study. *J Orthop Res*. 2012;30:1577-1580.

52. Kirby KN, Gerlanc D. BootES: an R package for bootstrap confidence intervals on effect sizes. *Behav Res Methods*. 2013;45:905-927.

53. R: The R Project for Statistical Computing. Available at: https://www.r-project.org/. Accessed April 1, 2016.

54. Yukawa Y, Kato F, Suda K, Yamagata M, Ueta T, Yoshida M. Normative data for parameters of sagittal spinal alignment in healthy subjects: an analysis of gender specific differences and changes with aging in 626 asymptomatic individuals. *Eur Spine J*. 2018;27:426-432.

55. Noshchenko A, Hoffecker L, Cain CMJ, Patel VV, Burger EL. Spinopelvic parameters in asymptomatic subjects without spine disease and deformity: a systematic review with meta-analysis. *Clin Spine Surg*. 2017;30:392-403.

56. Oskouian RJ, Shaffrey CI. Degenerative lumbar scoliosis. *Neurosurg Clin North Am*. 2006;17:299-315, vii.

57. Vos T, Flaxman AD, Naghavi M, et al. Years lived with disability (YLDs) for 1160 sequelae of 289 diseases and injuries 1990-2010: a systematic analysis for the Global Burden of Disease Study 2010. *Lancet*. 2012;380:2163-2196.

58. Trobisch PD, Hwang SW, Drange S. PSO without neuromonitoring: analysis of peri-op complication rate after lumbar pedicle subtraction osteotomy in adults. *Eur Spine J*. 2016;25:2629-2632.

59. Anwar HA, Butler JS, Yarashi T, Rajakulendran K, Molloy S. Segmental Pelvic Correlation (SPeC): a novel approach to understanding sagittal plane spinal alignment. *Spine J*. 2015;15:2518-2523.

60. Boissière L, Bourghli A, Vital J-M, Gille O, Obeid I. The lumbar lordosis index: a new ratio to detect spinal malalignment with a therapeutic impact for sagittal balance correction decisions in adult scoliosis surgery. *Eur Spine J*. 2013;22:1339-1345.

61. Been E, Barash A, Marom A, Kramer PA. Vertebral bodies or discs: which contributes more to human-like lumbar lordosis? *Clin Orthop*. 2010;468:1822-1829.

62. Garbossa D, Pejrona M, Damilano M, Sansone V, Ducati A, Berjano P. Pelvic parameters and global spine balance for spine degenerative disease: the importance of containing for the well being of content. *Eur Spine J*. 2014;23(suppl 6):616-627.

63. Smith JS, Shaffrey E, Klineberg E, et al. Prospective multicenter assessment of risk factors for rod fracture following surgery for adult spinal deformity. *J Neurosurg Spine*. 2014;21:994-1003.

64. Hallager DW, Gehrchen M, Dahl B, et al. Use of supplemental short pre-contoured accessory rods and cobalt chrome alloy posterior rods reduces primary rod strain and range of motion across the pedicle subtraction osteotomy level: an in vitro biomechanical study. *Spine*. 2016;41:E388-E395.

65. Charosky S, Moreno P, Maxy P. Instability and instrumentation failures after a PSO: a finite element analysis. *Eur Spine J*. 2014;23:2340-2349.

66. Deviren V, Tang JA, Scheer JK, et al. Construct rigidity after fatigue loading in pedicle subtraction osteotomy with or without adjacent interbody structural cages. *Glob Spine J*. 2012;2:213-220.

67. Luca A, Lovi A, Galbusera F, Brayda-Bruno M. Revision surgery after PSO failure with rod breakage: a comparison of different techniques. *Eur Spine J*. 2014;23(suppl 6):610-615.

68. Januszewski J, Beckman JM, Harris JE, Turner AW, Yen CP, Uribe JS. Biomechanical study of rod stress after pedicle subtraction osteotomy versus anterior column reconstruction: a finite element study. *Surg Neurol Int*. 2017;8:207.

69. Hyun S-J, Lenke LG, Kim Y-C, Koester LA, Blanke KM. Comparison of standard 2-rod constructs to multiple-rod constructs for fixation across 3-column spinal osteotomies. *Spine*. 2014;39:1899-1904.

70. Jager ZS, İnceoğlu S, Palmer D, Akpolat YT, Cheng WK. Preventing Instrumentation Failure in Three-Column Spinal Osteotomy: Biomechanical Analysis of Rod Configuration. *Spine Deform*. 2016;4:3-9.

71. Scheer JK, Tang JA, Deviren V, et al. Biomechanical analysis of revision strategies for rod fracture in pedicle subtraction osteotomy. *Neurosurgery*. 2011;69:164-172 [discussion 172].

72. Dick JC, Bourgeault CA. Notch sensitivity of titanium alloy, commercially pure titanium, and stainless steel spinal implants. *Spine*. 2001;26:1668-1672.

73. Barrey C, Perrin G, Michel F, Vital J-M, Obeid I. Pedicle subtraction osteotomy in the lumbar spine: indications, technical aspects, results and complications. *Eur J Orthop Surg Traumatol*. 2014;24(suppl 1):S21-S30.

74. Yu B-S, Zhuang X-M, Zheng Z-M, Li Z-M, Wang T-P, Lu WW. Biomechanical advantages of dual over single iliac screws in lumbo-iliac fixation construct. *Eur Spine J*. 2010;19:1121-1128.

75. Dahl BT, Harris JA, Gudipally M, Moldavsky M, Khalil S, Bucklen BS. Kinematic efficacy of supplemental anterior lumbar interbody fusion at lumbosacral levels in thoracolumbosacral deformity correction with and without pedicle subtraction osteotomy at L3: an in vitro cadaveric study. *Eur Spine J*. 2017;26:2773-2781.

76. Lehman RA, Kang DG, Wagner SC, et al. Biomechanical stability of transverse connectors in the setting of a thoracic pedicle subtraction osteotomy. *Spine J*. 2015;15:1629-1635.

77. Chang T-L, Sponseller PD, Kebaish KM, Fishman EK. Low profile pelvic fixation: anatomic parameters for sacral alar-iliac fixation versus traditional iliac fixation. *Spine*. 2009;34:436-440.

78. Nguyen T-Q, Buckley JM, Ames C, Deviren V. The fatigue life of contoured cobalt chrome posterior spinal fusion rods. *Proc Inst Mech Eng [H]*. 2011;225:194-198.

79. Fleischer GD, Kim YJ, Ferrara LA, Freeman AL, Boachie-Adjei O. Biomechanical analysis of sacral screw strain and range of motion in long posterior spinal fixation constructs: effects of lumbosacral fixation strategies in reducing sacral screw strains. *Spine*. 2012;37:E163-169.

80. Tang JA, Leasure JM, Smith JS, Buckley JM, Kondrashov D, Ames CP. Effect of severity of rod contour on posterior rod failure in the setting of lumbar pedicle subtraction osteotomy (PSO): a biomechanical study. *Neurosurgery*. 2013;72:276-282 [discussion 283].

81. Yao Z, Zheng G, Zhang Y, et al. Selection of lowest instrumented vertebra for thoracolumbar kyphosis in ankylosing spondylitis. *Spine*. 2016;41:591-597.

82. Bridwell KH, Lewis SJ, Edwards C, et al. Complications and outcomes of pedicle subtraction osteotomies for fixed sagittal imbalance. *Spine*. 2003;28:2093-2101.

83. Voyadzis J-M, Gala VC, O'Toole JE, Eichholz KM, Fessler RG. Minimally invasive posterior osteotomies. *Neurosurgery*. 2008;63(3 suppl):204-210.

Conflict of interest statement: The authors declare that the article content was composed in the absence of any commercial or financial relationships that could be construed as a potential conflict of interest.

Received 8 September 2018; accepted 7 November 2018

Citation: World Neurosurg. (2019) 123:e85-e102.
https://doi.org/10.1016/j.wneu.2018.11.052

Journal homepage: ***www.journals.elsevier.com/world-neurosurgery***

Available online: ***www.sciencedirect.com***